Icarus **160**, 32–43 (2002)
doi:10.1006/icar.2002.6935

The Existence of a Planet beyond 50 AU and the Orbital Distribution of the Classical Edgeworth–Kuiper-Belt Objects

A. Brunini

Observatorio Astronómico, Universidad Nacional de La Plata, Paseo del Bosque S/N, 1900 La Plata, Argentina; and CONICET, Avenida Rivadavia 1917, CP C1033AAJ, Ciudad de Buenos Aires, Argentina

and

M. D. Melita

Astronomy Unit, School of Mathematical Sciences, Queen Mary, University of London, Mile End Road, London E1 4NS, United Kingdom
E-mail: M.D.Melita@qmul.ac.uk

Received July 12, 2001; revised May 23, 2002

We study the effects of a Mars-like planetoid with a semimajor axis at about ∼60 AU orbiting embedded in the primordial Edgeworth–Kuiper belt (EKB). The origin of such an object can be explained in the framework of our current understanding of the origin of the outer Solar System, and a scenario for the orbital transport mechanism to its present location is given. The existence of such an object would produce a gap in the EKB distribution with an edge at about 50 AU, which seems to be in agreement with the most recent observations. No object at low eccentricity with semimajor axis beyond 50 AU has been detected so far, even though the present observing capabilities would allow an eventual detection (B. Gladman *et al.* 1998, *Astron. J.* 116, 2042–2054; D. Jewitt *et al.* 1998, *Astron. J.* 115, 2125–2135; E. I. Chiang and M. E. Brown 1999, *Astron. J.* 118, 1411–1422; R. L. Allen *et al.* 2000, *Astrophys. J.* 549, 241–244; C. A. Trujillo *et al.* 2001, *Astron. J.* 122, 457–473; B. Gladman *et al.* 2001, *Astron. J.* 122, 1051–1066; C. A. Trujillo and M. E. Brown 2001, *Astrophys. J.* 554, 95–98). Finally, ranges for the magnitude and proper motion of the proposed object are given.

Key Words: **Kuiper belt objects; comets, dynamics; comets, origin; origin, Solar System.**

1. INTRODUCTION

Since the discovery of the first Edgeworth–Kuiper belt object (EKBO) in 1992 (Jewitt and Luu 1993) the orbital distribution in the transneptunian region has gradually being known. Some ∼500 objects have been discovered at present (see Fig. 1). Their orbits can be divided into three different groups (Trujillo *et al.* 2001)[1]: (1) The first is the "classical" EKBOs (CEKBOs) with semimajor axes between 41 and 46 AU and moderate to low eccentricities ($e, i, 0.25$). Two-thirds of the objects belong to this group. (2) The resonant EKBOs (REKBOs) occupy the exterior mean-motion resonances (MMR) with Neptune. Most of them are trapped in the 2 : 3 MMR at ≈39.4 AU, the so-called "Plutinos," and also a few of them are located at the distant 1 : 2 NMMR (≈47.8 AU). This class comprises some 20% of the total. (3) The "scattered" EKBOs (SEKBOs) follow large eccentric orbits with $a \sim 90$ AU and $e \sim 0.6$, presumably due to their close interaction with Neptune (Duncan and Levison 1997). Their perihelia are clustered around 35 AU, although some with greater perihelion distances exist (Gladman *et al.* 2002). A few tens of objects of this class are known, representing some 10% of the total, but this population may outnumber the classical EKBOs.

The observations would indicate the presence of $\approx 10^5$ objects with diameter greater than 100 km orbiting the Sun between 30 and 50 AU with a combined mass of approximately $0.1 M_\oplus$.

A puzzling feature of the currently observed distribution is that no classical EKBO has been discovered with a semimajor axis beyond 50 AU (Gladman *et al.* 1998, 2001; Jewitt *et al.* 1998; Chiang and Brown 1999; Allen *et al.* 2001; Trujillo *et al.* 2001; Trujillo and Brown 2001), although an eventual detection would be within the reach of these surveys. Objects with the correspondent sky-plane velocities and apparent magnitudes should have been detected, and indeed, distant objects at equivalent heliocentric distances have already been observed in the scatter disk. If it is assumed that the Edgeworth–Kuiper belt (EKB) would extend up to ∼200 AU, Monte-Carlo simulations of EKBO discoveries as a function of heliocentric distance would yield some 40% of the objects to be discovered beyond 50 AU (Jewitt *et al.* 1998). While extrapolations based on the decay of the surface density of the primordial solar nebula would predict that some 10% of the total discoveries in the transneptunian region should be composed of objects at heliocentric

[1] A more detailed classification can be found in Gladman *et al.* (2001).

0019-1035/02 $35.00

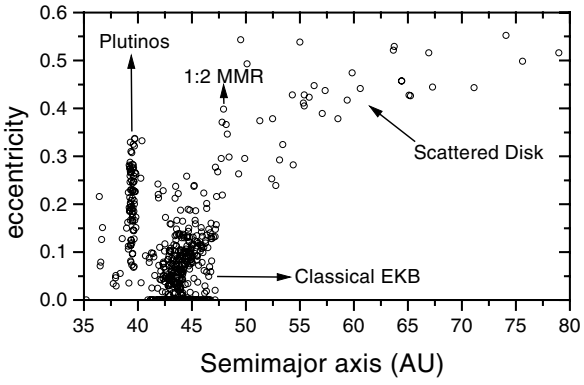

FIG. 1. The transneptunian region. Eccentricity vs semimajor axis of all the discovered objects detected in two or more oppositions, according to the Minor Planet Center. The three distinct populations are indicated.

distances beyond 50 AU (Chiang and Brown 1999), which at present time should sum up to some 30 objects, in the present observational sample there are none.

A number of hypotheses can be put forward to explain this feature. The maximum size of the objects may decrease with distance; however, the rate of decrease should be so large that such an effect would not be physically plausible (Jewitt *et al.* 1998, Trujillo *et al.* 2001). On the other hand, the primordial solar nebula might have had its exterior edge at those distances, depleting the region of material for objects to be formed; however, present observations of circumstellar disks indicate that it would have extended well beyond, from hundreds to thousands of astronomical units (Beckwith and Sargent 1996). It has also been argued that the interaction between the EKB disk and a passing star would leave noticeable signatures in the distribution, e.g., the orbital excitation observed in the inner belt (Brunini and Fernández 1996, Ida *et al.* 2000, de la Fuente Marcos and de la Fuente Marcos 2001). The truncation of the outer disk would be a natural by-product of such an encounter; however, the observed orbital distribution may be too steep to have been produced by a realistic stellar encounter (J. Larwood 2002, private communication).

In any case, the depletion of CEKBOs beyond the 1 : 2 NMMR has aroused some debate (Gladman *et al.* 1998, Trujillo *et al.* 2001). If the cumulative luminosity function, and hence the size distribution derived from it, is steep, then there are fewer large distant objects to be found, and the radial distances at which the objects are detected will be strongly biased toward the Sun. Some of the most recent observational work (Chiang and Brown 1999, Trujillo *et al.* 2001, Allen *et al.* 2001) prefer a shallower luminosity function with a power-law differential size distribution index of $q \approx 4$, while others (Gladman *et al.* 2001) argue that the number of faint objects have been underestimated by other authors, implying a steeper luminosity function ($q \approx 4.65$) and less distant objects to be observed; however, this argument has been recently challenged (Trujillo *et al.* 2001). In any case, there is still quite a lot of room for uncertainties regarding the problem. Nevertheless, it should be noted that the argument regarding the slope of the size distribution would not explain why most of the findings at heliocentric distances greater than 47 AU correspond to very eccentric orbits, unless the size distribution of the SEKBOs is very different from that corresponding to the CEKBOs, which would, perhaps, imply a different dynamical origin.

In this article we argue that the presence of a massive body beyond 50 AU would naturally explain the lack of objects in nearly circular orbits at greater distances. In Section 2 we show the effects of the perturbations on the native EKBOs produced by a small planet under different conditions. In Section 3 we put forward a plausible transport mechanism for that sort of objects from the outer planetary region to its hypothetical present state. Finally in Section 4 we compute possible values of its apparent magnitude and sky-plane proper motion, and we discuss several implications of the existence of this object.

2. THE FORMATION OF A GAP IN THE CLASSICAL BELT AND THE PRESENCE OF A PLANET

A massive object, with semimajor axis at about ∼60 AU, orbiting at low to moderate eccentricity, could provide the proper perturbation, through low-velocity encounters, to the resident primordial EKBOs, such that they leave the region in a time scale shorter than the age of the Solar System. Since there is no known mechanism that could remove the object from beyond 50 AU at low or moderate eccentricities, the object should still be orbiting there; however, it should be of small size—or in a very inclined orbit—or otherwise it would have been already detected.

A number of numerical simulations have been performed, where a massive object orbits while embedded in a swarm of test particles representing the primordial EKB. As we are mainly interested in the effects of the small planet on the test particles, we included only Neptune in our integrations, given that beyond 50 AU the belt is practically not sensitive dynamically to the rest of the planetary system. The test particles were distributed between 35 and 90 AU in near-circular orbits at low inclinations ($\leq 1^\circ$). The numerical integrator used is an updated version of the hybrid symplectic second-order method already used in Melita and Brunini (1999); in the present version the computation of the close encounters is solved by a Burlish and Stoer integrator. Several numerical tests indicated that this integrator is as accurate as other available integration packages (a ready-to-run version of the code is available at `http://heavy.fisica.edu.uy/~gallardo/evorb.html`, test runs can be found in the Appendix). The step size corresponding to the numerical experiments reported here is 5 year.

In the first set, the semimajor axis and eccentricity of the planetoid are set equal to 62 AU and 0.18, respectively, and its inclination to 1°; the mass of the planetoid ranges from $0.01 M_\oplus$ to $0.1 M_\oplus$. The end state of the system after 1 Gyr is shown in Fig. 2. Under these conditions, the orbital excitation necessary to produce a depletion of cold orbits at about 50 AU is

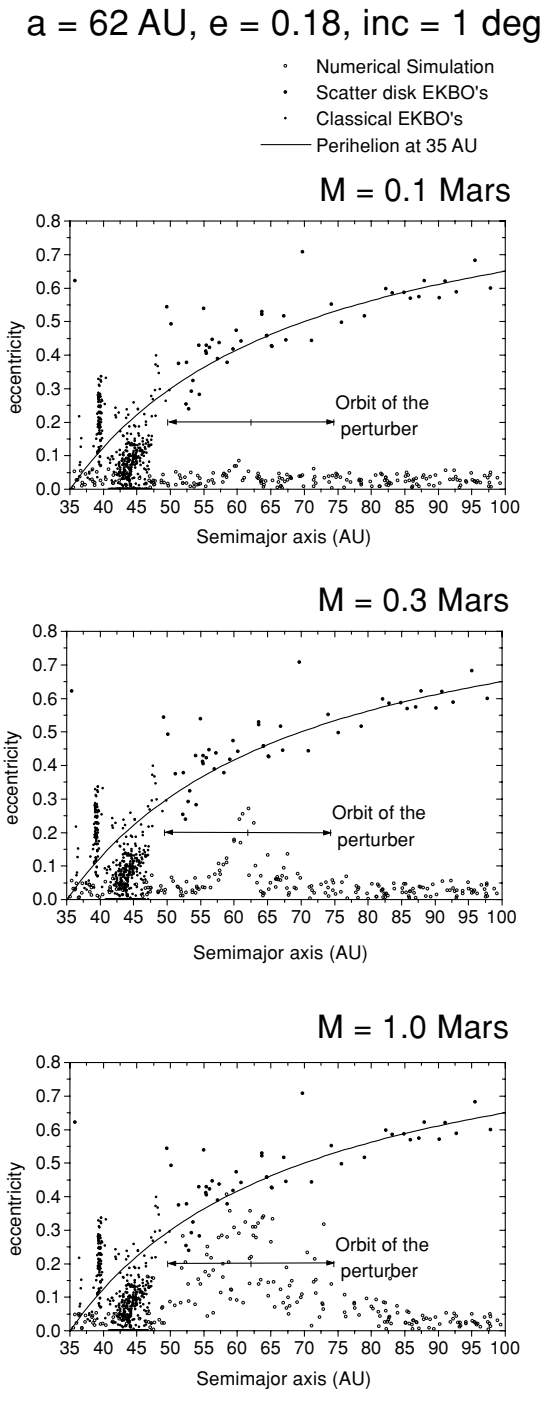

FIG. 2. Effect of a massive body at semimajor axis 62 AU, eccentricity 0.18, and inclination 1°. Masses are indicated in each case. Eccentricity vs semimajor axes of the observed EKBOs and the end states of the test particles after 1 Gyr.

only achieved in the case where the object is the most massive. However, the orbital distribution does not match very closely the observations, in particular with respect to the inclination distribution (see Fig. 3), which may suggest that the perturbing agent is in an inclined orbit.

In the following simulation the semimajor axis and eccentricity of the planetoid are set equal to 60 AU and 0.2 and its inclination to 10° (see Fig. 4). Although this case gives a better match, the depletion of observed cold orbits seems to be more steep, almost indicating an *edge*, which may suggest that the perturber is either closer and/or more massive.

In the final set, the semimajor axis of the planetoid is set equal to 56 AU, the eccentricity to 0.1, and the inclination to 10°. Figure 5 shows a run-in with a planetoid mass of $0.1M_{\oplus}$. Although the observed *edge* at ≈50 AU is well reproduced, there are a number of objects remaining at moderate eccentricities beyond, and hence it can be argued that those could have been already detected. However, if their orbits are also inclined, their detectability would be biased against their discovery.

If the mass of the planetoid is set equal to $0.2M_{\oplus}$, a remarkable match with the observed distribution is obtained in both eccentricities and inclinations (see Fig. 6). The eccentricity excitation suffered by the native EKBOs is shown in Fig. 7 for the last case. As a consequence, a noticeable depletion of nearly circular objects is produced (see Fig. 8); the almost total absence

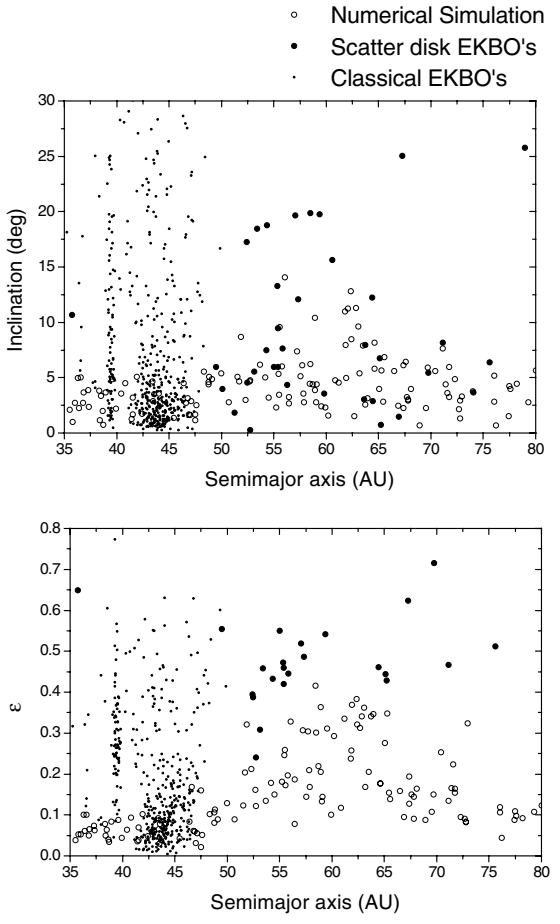

FIG. 3. Effect of a body of mass $0.1M_{\oplus}$, semimajor axis at 62 AU, eccentricity 0.18, and inclination 1°. Inclination vs semimajor axis of the test particles after 1 Gyr and observed EKBOs.

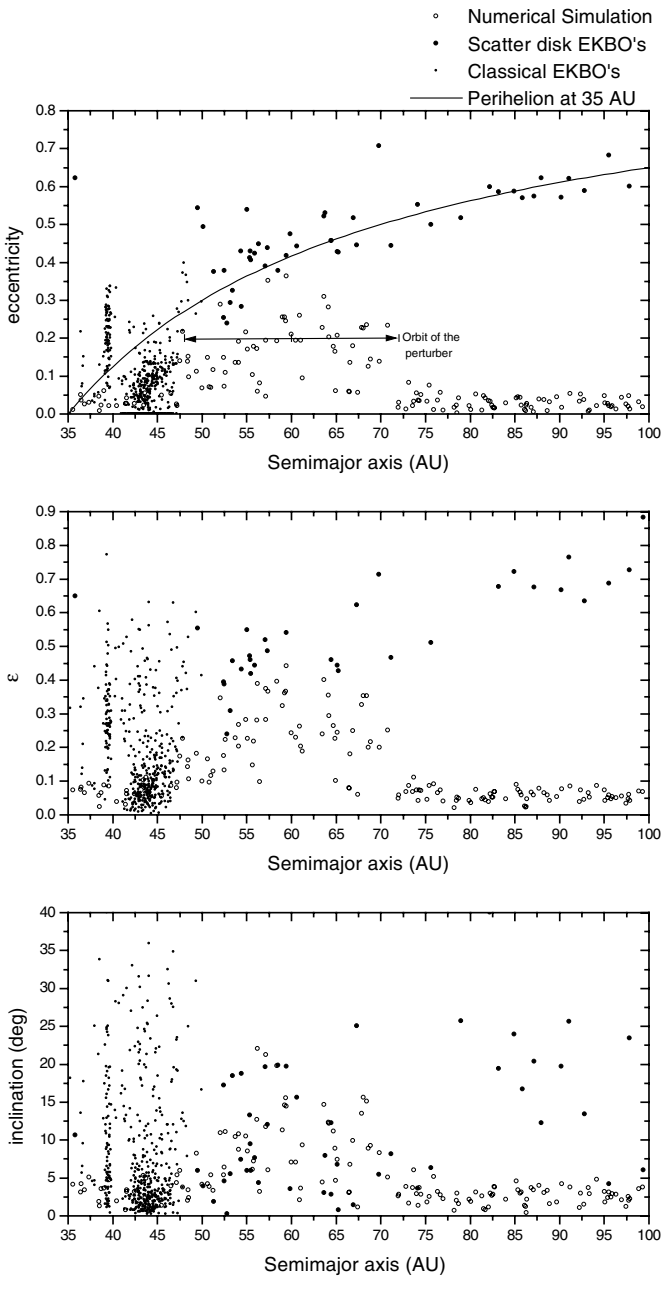

FIG. 4. Effect of a massive body of mass $0.1M_\oplus$ at semimajor axis 60 AU, eccentricity, $e = 0.2$ and inclination, $i = 10^\circ$. Eccentricity, inclination, and $\varepsilon = (e^2 + i^2)^{1/2}$ vs the semimajor axis of the observed EKBO's and the end states of the test particles after 1 Gyr.

of low-eccentricity objects can be due to the action of secular resonance with the planetoid, which can affect the orbit more than mere gravitational stirring.

Naturally there are a number of effects that would enhance the depletion effect of the planet. If the planet would have migrated, then the excitation (both local and remote) is produced throughout the migrated region. To illustrate the effect we have performed a simulation where a planet with the same mass and eccentricity as in the first set of simulations migrated its semimajor axis only between $t_1 = 60$ and 80 Myr from 55 to 75 AU at a rate of $\dot{a} = 10^{-8}$ AU/yr. As the scope of this run was to asses the possible effect of planet migration, the migration rate $\dot{a}$ was assumed uniform in time. After each time step of our symplectic integration the semimajor axis of the planet was updated according to this migration rate. The end state of the system after 1 Gyr is shown in Fig. 9.

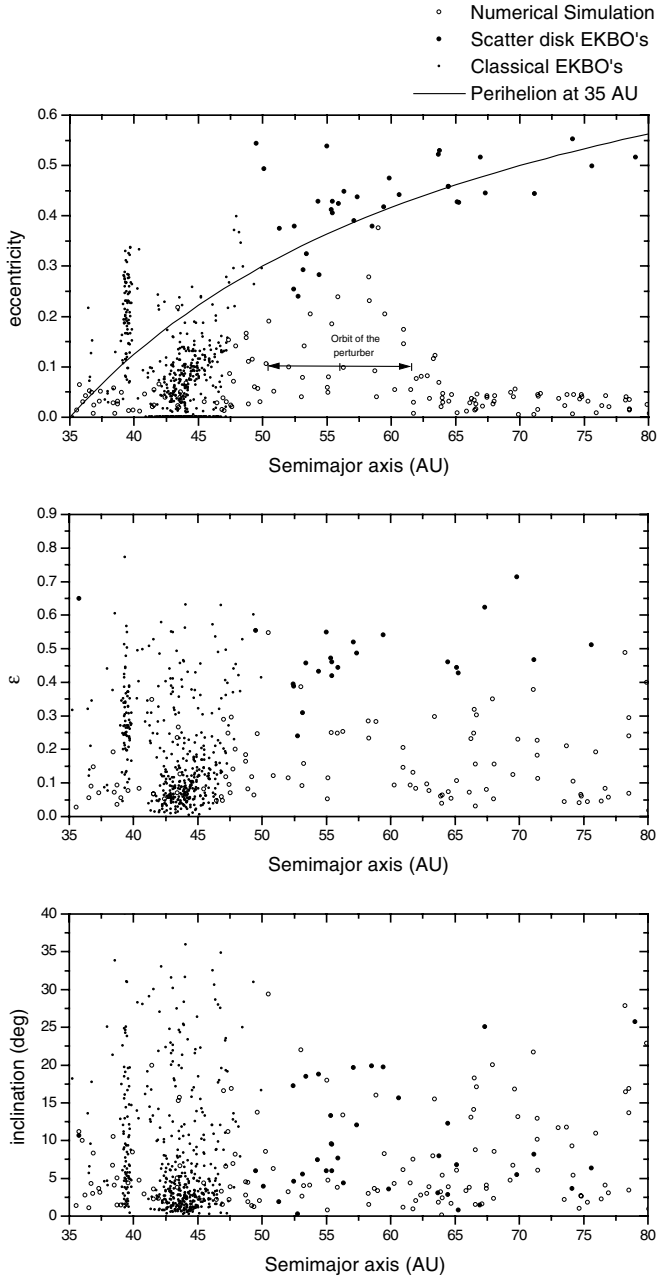

FIG. 5. Effect of a massive body of mass $0.1M_\oplus$ at semimajor axis, 56 AU, eccentricity, $e = 0.1$ and inclination, $i = 10^\circ$. Eccentricity, inclination, and $\varepsilon = (e^2 + i^2)^{1/2}$ vs the semimajor axis of the observed EKBOs and the end states of the test particles after 1 Gyr.

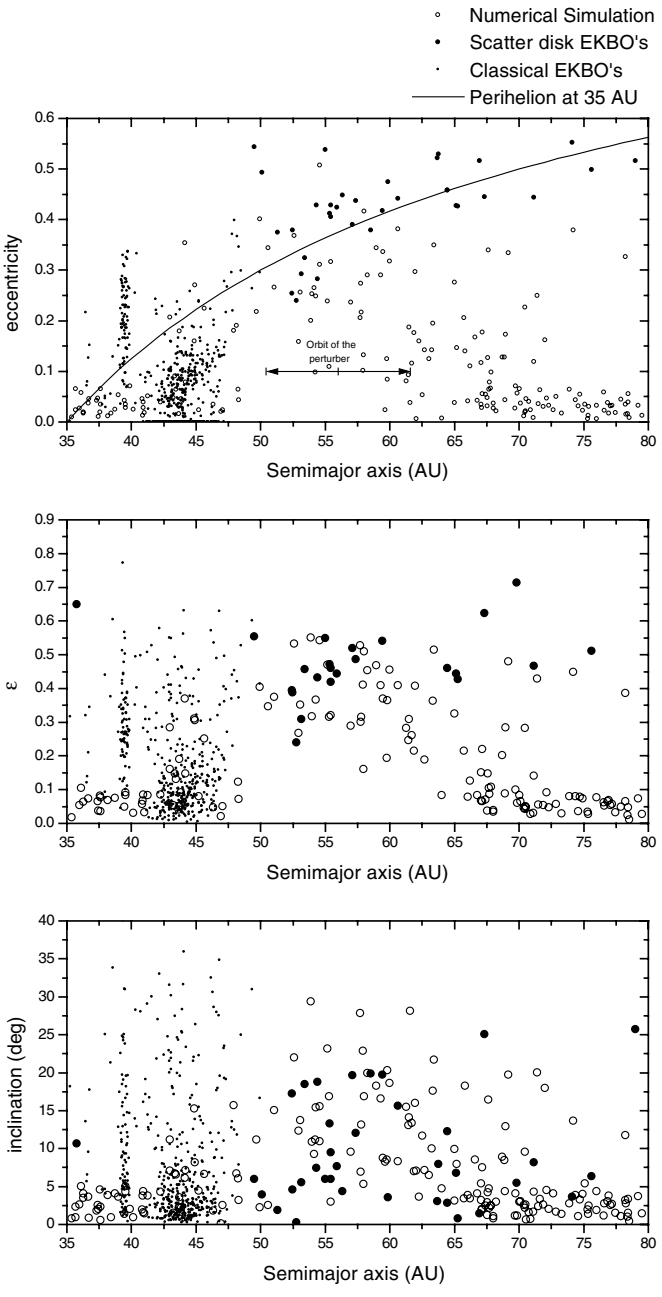

FIG. 6. Effect of a massive body of mass $0.2M_\oplus$ at semimajor axis 56 AU, eccentricity, $e = 0.2$, and inclination, $i = 10^\circ$. Eccentricity, inclination and $\varepsilon = (e^2 + i^2)^{1/2}$ vs the semimajor axis of the observed EKBOs and the end states of the test particles after 1 Gyr.

2.1. The Transplutonian Planet and the Resonant EKBOs

It should be noted that the Plutinos with the most eccentric orbits have their aphelia at ≈53 AU. Thus, since the massive objects described above have perihelia at ≈50 AU, it can be argued that the planetoid would disrupt the population at the 2 : 3 exterior MMR with Neptune. To determine whether the perturbative effects on the resonant EKB distribution would rule out

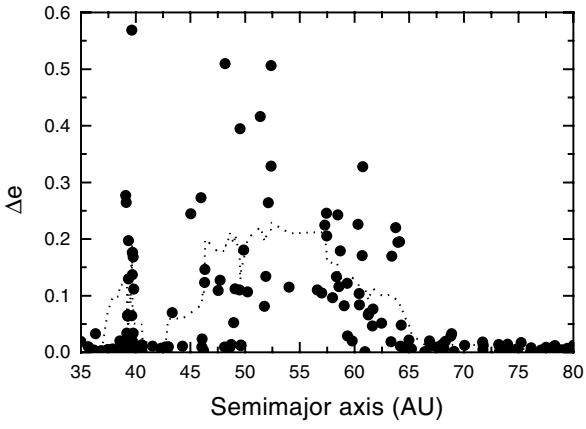

FIG. 7. Effect of a body of mass $0.2M_\oplus$ semimajor axis, eccentricity 0.1, and inclination 10°. Eccentricity change of the test particles after 1 Gyr. The dotted line corresponds to a smoothed interpolation by adjacent averaging.

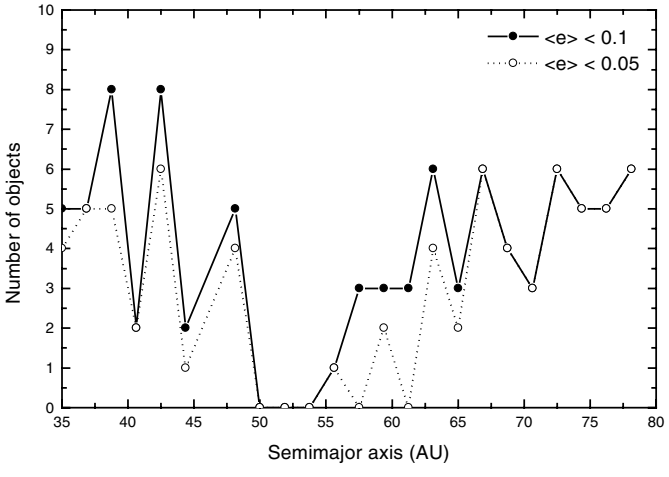

FIG. 8. Effect of a body of mass $0.2M_\oplus$, semimajor axis 56 AU, eccentricity 0.1, and inclination 10°. Number of test particles with eccentricities below 0.1 and 0.05 after 1 Gyr.

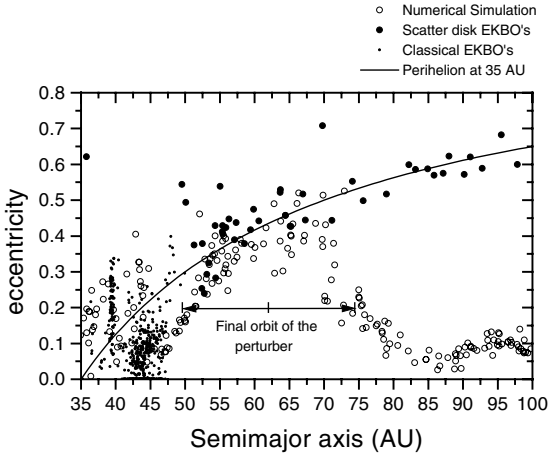

FIG. 9. Effect of a body of mass $0.1M_\oplus$ with a migrating semimajor axis from 55 to 75 AU and eccentricity 0.2. Eccentricity vs the semimajor axis of the observed scattered EKBOs and the end states of the test particles after 1 Gyr.

TABLE I

Percentage of Bodies Remaining within the Resonance 2 : 3 Neptune MMR and Maximum Final Eccentricities of the Plutino Population for Different Perturbing Objects

Mass ($M_\oplus$)	a (AU)	e	Remaining (%) bodies	Max. final e
—	—	—	98.1	0.35
0.3	56.0	0.1	51.9	0.2
0.3	60.0	0.2	44.2	0.2
0.2	56.0	0.1	61.5	0.3
0.1	56.0	0.1	84.6	0.3
0.1	60.0	0.2	73.1	0.4

Note. The inclination of the planetoids have been set equal to 10°. The first file corresponds to the case where the only perturber present is Neptune.

the existence of such a massive object, we have performed some numerical simulations. The orbits of 52 test particles initially residing inside the 2 : 3 Neptune MMR are integrated for 1 Gyr in the presence of the outermost major planet and a massive object. The initial orbital parameters of the test particles were chosen to be equal to those of the currently observed Plutinos that satisfy the stability rule given by Yu and Tremaine (1999). The number of objects of this *Plutino population* remaining bounded to the 2 : 3 NMMR and their maximum final eccentricities for different parameters of the perturbing agent are given in Table I. It is apparent that the planetoid perturbs significantly the Plutino population over the age of the Solar System if its mass is greater than $0.2M_\oplus$. However, in this case, it still plays a role in the orbital history of the 2 : 3 MMR population. If the Plutinos observed at eccentricities ≈0.35 are not in a transient state, then the mass of the transplutonian planet can be constrained to be no greater than $0.1M_\oplus$.

3. A POSSIBLE ORIGIN FOR THE "TRANSPLUTONIAN PLANET"

Beyond 50 AU, Neptune's gravitational perturbations are negligible (Duncan *et al.* 1995), and indeed it has been shown that no first-order secular resonances can be found beyond ≈42 AU (Kenzévic *et al.* 1991). Although the EKB cannot be considered collisionless before ∼75 AU (Stern and Colwell 1997a), self-interactions on their own would not be sufficient to clear a region populated by cold orbits (Davis and Farinella 1997, Kenyon and Luu 1999). However, the structure of the inner EKB would have been heavily perturbed during the formation of the outer planets (Malhotra 1995, Morbidelli and Valsechi 1997, Melita and Brunini 1999, Nagasawa and Ida 2000). In the latest stage of the formation of the Solar System, the masses of Uranus and Neptune would have grown by the concurrent pairwise accretion of massive planetesimals (Fernández and Ip 1984, 1996; Brunini and Fernández 1999). This process is highly inefficient and a great deal of mass would have been expelled from the system. As a consequence, a number of small protoplanets would have invaded the transneptunian region. Some features of the currently observed orbital distribution of EKBOs can be regarded as a fossil record of such an invasion. Evidence of the existence of a primordial population of massive objects in the region (Stern 1991, Parisi and Brunini 1999) can be the rather high mean eccentricities of the classical EKBOs, the very low number of objects in the cold stable regions with semimajor axes between 36 and 39 AU, the tilt of the spin axis of Uranus, the retrograde orbit of Triton, and the existence of the binary Pluto–Charon. Planetary migration could also have shaped the EKB distribution noticeably (Malhotra 1995). Also the shape of the inclination distribution of the classical belt and its correlation with the color and size distributions suggest that these populations are *contaminated* by objects originating further in the belt (Tegler and Romanishin 2000, Brown 2001, Levison and Stern 2001, Trujillo and Brown 2002).

For the EKBOs to grow up by binary accretion to the sizes currently observed, a disk two orders of magnitude more massive is required. Thus, the way by which most of the inner EKB has been lost should be understood. The inner region is affected greatly by self-collisions that, if the orbits are excited enough, could derive into a collisional cascade (Davis and Farinella 1997, Kenyon and Luu 1999, Stern and Colwell 1997b). Thus, the protoplanet invasion would certainly aid the putative mass depletion in the region (Morbidelli and Valsechi 1997, Melita and Brunini 1999).

Results from a set of self-consistent simulations of the evolution of the EKB at the time of the formation of the outermost planets (Melita and Brunini 1999) gave us a clue to understanding the origin of the "gap" at 50 AU observed in the distribution of classical EKBOs (see Fig. 10).

The simulations have been performed using a second-order symplectic map (Wisdom and Holman 1991). Details of the numerical code can be seen in the Appendix. In order to speed up the computational work, we have introduced some simplifying assumptions: In all the runs reported in this section, all objects suffer the perturbations of the planets. Mutual remote perturbations between the planetesimals are not considered; only close encounters are computed. If two objects enter within the range of mutual Hill's spheres, then the orbit is integrated as reported in the Appendix. Fragmentation has not been considered; all collisions lead to accretion. Although not completely accurate, our results have been instrumental in deriving a transport mechanism of a planetary body from the Uranus–Neptune region to a cold orbit in the EKB. These simulations are not intended to obtain any parameter quantitavely but to illustrate the transport process.[2]

[2] It should be noted that the numerical model used for these simulations is similar to that used by Brunini and Fernández (1999). However, in the present model, the maximum distance at which we compute close encounters is defined by a factor of the mutual Hill's radius. In the previous code the radius of the sphere of influence (Danby 1962) was used. In this integration method, the bodies do not "see" each other unless a close encounter occurs. In the hyperbolic

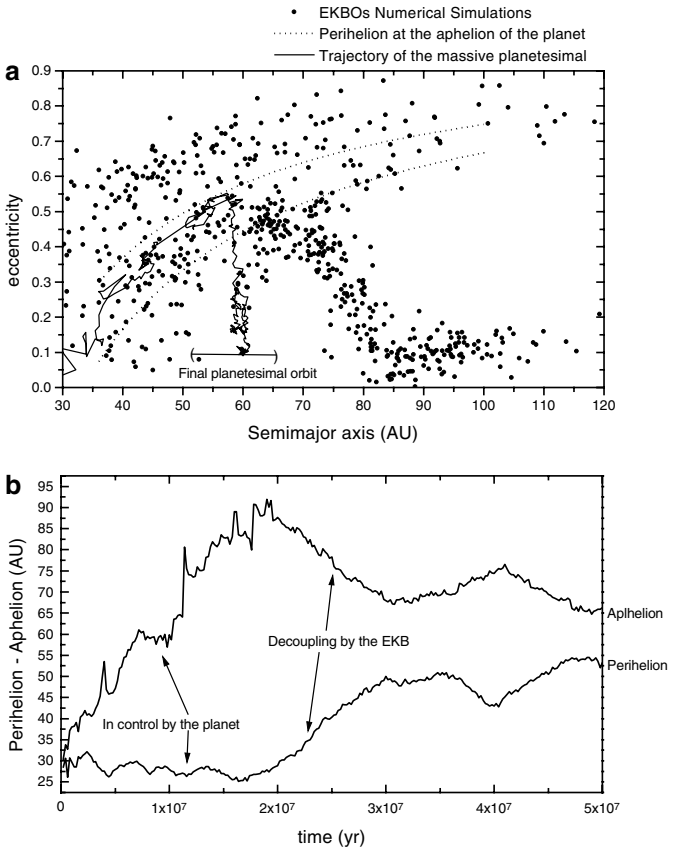

FIG. 10. Self-consistent numerical simulation of the evolution of the EKB during the formation of the outer planets. (a) Eccentricity vs semimajor axis of the native EKBOs. The dotted lines indicate the perihelia of the outermost planets. The trajectory of an invading planetesimal of mass $0.12 M_\oplus$ has also been plotted. (b) Evolution of the perihelion and aphelion distance of the invading planetesimal.

We started our simulations with only Saturn and Jupiter with their present masses and orbits defined as planets. Once an object grows greater than $1.5 \times 10^{-6} M_\odot$, it is included among the set of planets.

Two populations of planetesimals are initially set up with an r^{-2} distribution law, where r is the heliocentric distance. The first one, representative of the planetary-region planetesimals at the time of the beginning of the simulations, is placed between 12 and 35 AU and has a total mass equal to twice the sum of the masses of Uranus and Neptune distributed uniformly among 500 particles. The other population, to which we will refer to as the *belt population*, represents bodies existing in the inner Kuiper belt. It extends between 35 and 100 AU and consists of a number of Pluto's mass bodies. Both populations are initially uniformly distributed at low eccentricities and inclinations. The inner particles have a typical density of rocky materials (2 g cm^{-3}) and the outer particles have an icy density (0.5 g cm^{-3}).

The most relevant parameters of each run are shown in Table II.

It is apparent that the planetary bodies formed in the Uranus–Neptune region are much smaller than the actual outer planets. Regardless of the cause, if these results are genuine, they could be calling for a physical cause for the enhancement of the protoplanetary cross sections. This enhancement can be produced by the presence of a gaseous envelope around massive planetesimals (Stevenson 1982, 1984) in the Uranus–Neptune region (Brunini and Melita 2002), where Uranus- and Neptune-like objects can grow under these conditions. On the other hand, alternative scenarios are also possible; for example, the cores of Uranus and Neptune may have originated in a region further in (Thomes *et al.* 1999).

In some of these simulations, massive planetesimals expelled from the planetary region by the action of Neptune follows a distinctive dynamical route that has a remarkable effect on the EKB distribution (see Fig. 10). When a massive object is taken in control by Neptune, the major perturbations on its orbit occur when the planetesimal encounters the planet at perihelion. By the transfer of orbital energy and angular momentum its aphelion increases while its periapsis remains nearly fixed. As its orbit expands, the object immerses itself into the primordial EKB. The interaction with the native EKBOs, acting as a drag, reduces its eccentricity by the exchange of orbital angular momentum, thus decoupling its perihelion from the Neptune region, until it is finally released from the control of the planet. A similar mechanism has been described for a planetary core originating in the Jupiter–Saturn region as an alternative scenario for the formation of Uranus and Neptune (Thomes *et al.* 1999). While and after the massive object is being decoupled, the orbits of the surrounding native EKBOs are being heavily perturbed by close encounters with it. The effect on the overall transneptunian distribution can be readily seen in Fig. 11, where gaps at low eccentricity are cleared and the objects removed from that region evolve into higher eccentricity—more unstable—orbits. The inclination of the invading objects are above the mean inclination of the primordial EKB distribution, but they all still remain close to their very low initial inclination.

Naturally, the objects removed from the classical EKB could also reach the dynamical control of Neptune, hence contributing to the population of the scatter disk, and perhaps some invading objects could be found today amongst the more excited objects within the classical belt (Tegler and Romanishin 2000, Brown 2001, Levison and Stern 2001, Trujillo and Brown 2002). In some of the runs more than one massive planetesimal have

approximation the velocity change increases with the relative velocity ad infinitum, which corresponds to the value when mutual interaction is negligible (i.e., at a *large mutual distance*). If the close encounter is defined at a smaller distance, all the mutual acceleration suffered while reaching that distance is lost. Then the relative speed would be smaller than it should have been and therefore there would be an overestimation of the gravitational cross section. If the bodies *start* seeing each other at a small distance, then the cross section grows. There was an artificial growth of the cross section for this reason in the previous code (Brunini and Melita 2002). As can be seen, the planetary bodies formed in the simulations presented here are much smaller than those in Brunini and Fernández (1999).

TABLE II
Some Initial and Final Parameters for Runs of the Model of Planetary Formation and Evolution of the Kuiper Belt Region

Run	Initial max. e	Initial max. inc. (rad)	No. of int.	No. of ext.	Formed planets	No. of small planets	Belt	
							Ext.	Int.
1	1×10^{-2}	1×10^{-2}	500	500	$m\,(M_\odot)$ 3.79×10^{-6} 1.91×10^{-6} a (AU) 23.48 34.54	1	468	109
2	1×10^{-2}	1×10^{-2}	500	600	$m\,(M_\odot)$ 3.82×10^{-6} a (AU) 30.96	1	554	107
3	1×10^{-3}	5×10^{-4}	500	600	$m\,(M_\odot)$ 1.59×10^{-6} 1.92×10^{-6} a (AU) 20.64 37.63	4	529	119
4	1×10^{-3}	5×10^{-4}	500	600	$m\,(M_\odot)$ 3.81×10^{-6} 2.67×10^{-6} a (AU) 25.25 33.33	4	526	91

Note. Small planets refer to bodies with masses greater than $1.5 \times 10^{-6}\,M_\odot$ with semi major axis in the belt region. The last columns indicate the number of objects remaining in the belt, discriminating between native and those that have invaded the region from the interior.

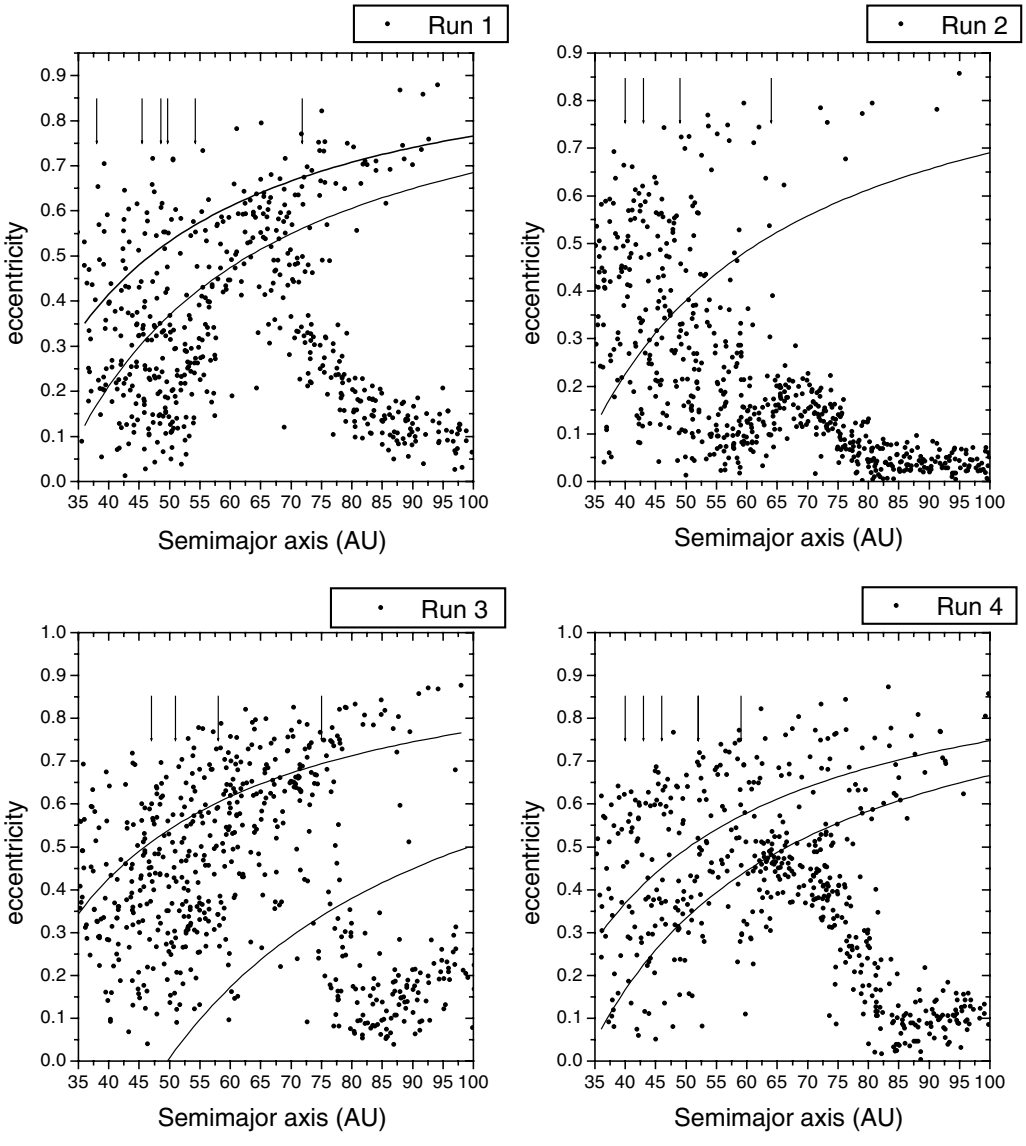

FIG. 11. Self-consistent numerical simulation of the evolution of the EKB during the formation of the outer planets. Eccentricity vs the semimajor axis of the native EKBOs for different runs. The solid lines indicate the perihelia of the outermost planets, and vertical markers indicate the location of their lowest-order mean-motion resonances.

invaded the belt (see Table II), which leaves open the possibility that the transneptunian belt could have been shaped by more than one planetoid.

4. DISCUSSION

The apparent magnitudes of bodies with the same radius and albedo as Pluto- and Mars-size bodies at 50 and 70 AU are given in Table III. Albedos have been assumed to be similar to that of Pluto (brightened by condensed ices over its surface) and those typical of short-period comets (similar to those observed in the EKBOs, Jewitt *et al.* 2001). A body's proper motion would be on the order of 1.89 arcsec/h. Although some recent surveys have their detection efficiency at about 100% for such luminocities, the slow proper motion at that distance can make eventual detection harder. On the other hand, the only large-scale survey to have reached magnitudes of $\sim$21 was that of Kowal (1989), which did not stray far beyond the ecliptic. Thus, if there is a planetary body beyond Pluto orbiting at a moderate or high inclination ($\geq 10^\circ$) or with a low cometary-like albedo, it would have remained undetected. It should be noted that the observed distribution is better matched when the perturber is in an inclined orbit. Regarding the origin of the inclination of this object, we expect planetesimals to be expelled close to its primordial plane, where most of the interaction with a forming planet takes place. However, under certain conditions, as it travels through the inner EKB, it may cross several secular resonances capable of exiting its inclination, as in the node resonance with Neptune. Perhaps the very low initial inclinations and the short time span of our accretion simulations conspired to hide this effect; however, it is a process that remains to be studied more carefully. Nevertheless, it should be noted that the more *inclined* population in the classical belt, related to the larger-sized objects, have been identified as the *invading* population (Levison and Stern 2001).

Naturally, the size of the gap cleared by such an object depends on the eccentricity of the planetoid. Thus, the tail of the EKB should continue some distance beyond its aphelion, so—if the body itself is not detected first—the eventual discovery of classical EKBOs at distances beyond the gap could be considered as independent evidence of its existence.

According to Trujillo and Brown (2001), The *cutoff* in the EKB would begin at $\sim$48 AU and the distribution could resume at $\sim$76 AU. Thus, a consistent value for the perihelion of the planetoid would be $\sim$49 AU and its aphelion $\sim$78 AU; then the corresponding semimajor axis would be $\sim$62 AU and the eccentricity $\sim$0.21. As mentioned above a large inclination would ensure that it remains undetected at present. The effect of such an object has been illustrated, and it would be *roughly* consistent with current observations. Although the SEKBO's sample is not large enough, if an eventual grouping in nodes and inclinations is detected in it, the corresponding values could give additional clues as to the orbital values of the planetoid.

If such an object is eventually observed—together with the EKBOs, centaurs, and comets—it would give important clues as to the study of the outer Solar System. Its crater record would tell us about the size distribution of the planetesimals that gave birth to the outer planets. The idea that the outer Solar System was once populated by a big number of massive objects (Fernández and Ip 1984, 1996; Stern 1991; Morbidelli and Valsechi 1997; Brunini and Fernández 1999; Melita and Brunini 1999; Parisi and Brunini 1999) would gain an independent and robust source of confirmation. It would also help to understand the origin and evolution of the scatter disk and the classical belt. If the object had been decoupled from Neptune by dynamical friction, as previously described, then some constraints on the primordial mass of the EKB can be drawn. The possibility that such an object has been formed *in situ* should not be ruled out, since aggregation studies in the region are consistent with that hypothesis under very favorable conditions (Stern and Colwell 1997b). Its existence is also consistent with the size distribution function resulting from the most recent surveys (Gladman *et al.* 1998, Jewitt *et al.* 1998, Chiang and Brown 1999, Sheppard *et al.* 2000). Moreover, the existence of SEKBOs with perihelion beyond the control of Neptune suggests a distant disturbing agent as that put forward in this work (Collander-Brown *et al.* 2001, Gladman *et al.* 2002). Thus, our results support the suggestion that Mars-like objects should be looked for in the transneptunian region (Chiang and Brown 1999, Gladman *et al.* 2002), and surveys in that direction are encouraged.

TABLE III
Visual Apparent Magnitudes as a Function of Albedo, p, Diameter, R, and Geocentric Distance, r

	$p = 0.04$		$p = 0.3$	
r (AU)	$R = 2000$ km	$R = 4000$ km	$R = 2000$ km	$R = 4000$ km
50	19.9	18.4	17.7	16.2
70	21.4	19.9	19.17	17.7

APPENDIX

The integration code used on this paper is based on the Wisdom and Holman (1991) second-order symplectic integrator implemented by Brunini and Melita (1998). We improved our previous code by including in the treatment of close encounters the strategy developed by Chambers (1999). In this Appendix, we present some of the most representative tests we have performed in order to asses the behavior of several parts of the code. The accuracy of the integration of the massive objects (planets) was checked by the evolution of its total energy, which remained nearly constant (it showed oscillations of one part in 10^{-9}) during a time span of 10^8 year, using a stepsize of 0.1 year.

A.1. Massless Particles and Planets

The accuracy of the integration of massless particles encountering a planet was estimated in several ways. A first approach was to check the evolution of the Jacobi constant in the frame of the restricted three-body problem. After several hundred encounters the particles can experience relative changes in the Jacobi constant on the order of 10^{-5} to 10^{-6}—at most—with a time step of $P/50$, where P is the revolution period of the planet, and this holds even for orbits with very small perihelion distances. Maximum changes of greater than

an order of magnitude can occur, but only if the particles have heliocentric orbital eccentricities of $e > 0.96$. The integrator was also tested by computing the orbital evolution of objects already studied by other authors and also by reproducing the circumstances of the next tow or three encounters of the Earth with some potential hazardous asteroids (PHA), as predicted on the JPL NEO Web site (neo.jpl.nasa.gov/neo/pha.html).

Some of the numerical tests presented in Chambers (1999) were performed with the same parameters (time steps and $r_{\rm crit}$). The first check (Chambers 1999, Sect. 5.2) was the integration of 36 massless particles in the field of the Sun and one planet. All the particles were placed in orbits with a semimajor axis of $a = 36$ AU, eccentricity $e = 0.18$, and orbital inclination $i = 0$. The mean anomalies were evenly spaced along their orbits. The corresponding elements for the planet were $a = 30$ AU, $e = 0$, and $i = M = 0$. The mass was that of Neptune. The system was integrated for 10^6 year. The maximum of the absolute value of the relative error in the Jacobi constant C of the particles was of one part in 10^{-7}. The general behavior of the Jacobi integral does not show secular trends.

A.2. Gravitational Focusing

Greenzweig and Lissauer (1990) have performed a careful analysis of the enhancement of the collision cross section of planetary bodies due to gravitational focusing. They integrated orbits of particles encountering a planet, under the gravitational attraction of the planet and the Sun. The planet, with mass $10^{-6}\ M_\odot$ was placed on a circular orbit. Its geometrical radius is chosen between two fixed values ($R = 0.1 R_{\rm H}$ or $R = 0.005 R_{\rm H}$, where $R_{\rm H}$ is its Hill's radius). Greenzweig and Lissauer (1990) performed several runs, each run being characterized by the initial eccentricity and inclination of the massless particles, which was the same for all of them. So we will identify each run by its eccentricity. The semimajor axes of the particles were spread in a region close to the planet. (For a complete description of the initial conditions of each run see Table 1 of Greenzweig and Lissauer 1990.) The result of each one of our runs was obtained integrating 10^5 particles through one close encounter with the planet, using a step size of 0.005 year. They are shown in Fig. 12, as the fraction of objects impacting the planet for each run. The agreement with the results of Greenzweig and Lissauer (1990) is quite good.

A.3. A Massive Planetary System

The test (Chambers 1999, Sect. 5.1) we present here consists of the numerical integration of the four giant planets with masses enhanced by a factor of 50, during a time interval of 1000 year, using a time step of 0.03 year. This represents the first check involving close encounters between massive bodies. In principle, it is not possible to reproduce exactly the behavior found in other simulations reported in the literature, because the system is extremely chaotic. Even though several close encounters occur between the planets, the total energy of the system remained bounded, and we did not observe any secular trend. The maximum (in absolute value) of the energy error found in our simulation was $(E - E_0)/E_0 = 1.67 \times 10^{-7}$, where E is the total energy of the system at a given time and E_0 is the same quantity at $t = 0$.

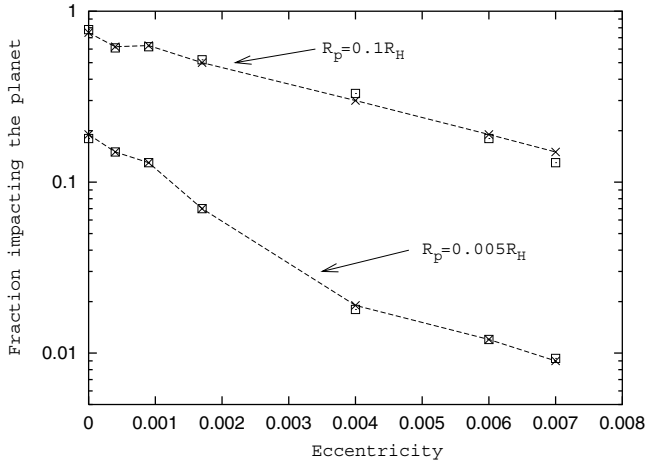

FIG. 12. The fraction of test particles that impact a planet as a function of the initial eccentricity of the particles. The physical radius of the planet $R_{\rm p}$ is given in terms of its Hill's radius $R_{\rm H}$. The dashed curves are lineal interpolations to the numerical values obtained by Greenzweig and Lissauer (1990) (crosses), whereas the results obtained with our code are represented by empty squares.

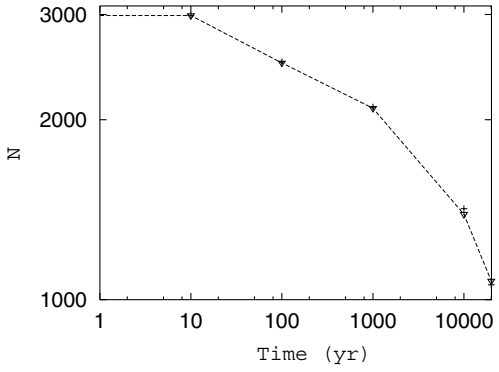

FIG. 13. Evolution of the number of planetesimals remaining in the simulation. The triangles connected by the dashed line is the result of Kokubo and Ida (1996). Our result is represented by the pluses.

A.4. Runaway Accretion

Kokubo and Ida (1996) performed 3-D N-body numerical simulations of planetary accretion, integrating the orbits of a large number of interacting equal-mass planetesimals with their fourth-order Hermite scheme with individual time steps. This problem was selected, in order to prove the efficiency of our code to predict close encounters and collisions and also to evaluate accretions. The initial conditions were taken from Kokubo and Ida (1996, Sect. 3.2). Three-thousand equal-mass (10^{23} g planetesimals were distributed in a ring of width 0.04 AU around 1 AU. Initial eccentricities and inclinations of the planetesimals were given by Gaussian distributions with dispersions of $\langle e^2\rangle^{1/2} = 2\langle i^2\rangle^{1/2} = 2R_{\rm H}/a$, $R_{\rm H}$ being the Hill's radius of the particles and a the semimajor axis. In order to reduce computation time Kokubo and Ida (1996) increased the physical radius of the planetesimals by a factor of 5. We used the same factor, assuming, as

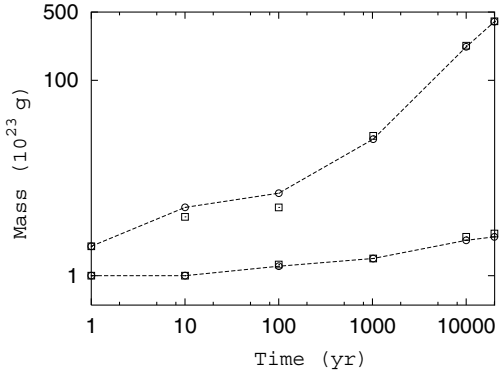

FIG. 14. The evolution of the mass of the largest body is compared with the mean mass of the rest of the population of planetesimals. The circles connected by the dashed line are the results from Kokubo and Ida (1996). Our results are represented by squares.

Kokubo and Ida (1996) had done, a mass density of the planetesimals equal to 2 g cm^{-3}. We integrated the system for a time span of 2×10^4 year, assuming perfect accretion, with a time step of 0.005 year. The comparison of the main results of our run with that of Kokubo and Ida (1996) are shown in Figs. 13 and 14. Figure 13 displays the number of bodies as a function of time. Figure 14 shows the evolution of the mass of the largest body, as compared to the evolution of the mean mass with the exception of the largest body. The agreement is very good. At the end of our simulation, the largest body becomes 402 times of its initial mass, whereas in Kokubo and Ida (1996) this figure is 398. The final r.m.s. eccentricity and inclination in our simulation is $\langle e^2 \rangle^{1/2} = 0.012$, $\langle i^2 \rangle^{1/2} = 0.05$ (very close to the final values in Kokubo and Ida's simulation). As expected, the ratio $\langle e^2 \rangle^{1/2} / \langle i^2 \rangle^{1/2}$ is near 0.5.

ACKNOWLEDGMENTS

We are grateful to A. Morbidelli and B. Gladman for their useful comments. M.D.M. thanks I. P. Williams, A. Fitzsimmons, and S. Collander-Brown for very enlightening discussions. We also thank the two anonymous referees whose comments have helped to improve greatly this manuscript. We acknowledge the financial support by IALP (CONICET).

REFERENCES

Allen, R. L., G. M. Bernstein, and R. Malhotra 2001. The edge of the Solar System. *Astrophys. J.* **549**, 241–244.

Beckwith, S. V. W., and A. I. Sargent 1996. Circumstellar disks and the search for neighboring planetary systems. *Nature* **383**, 139–144.

Brown, M. E. 2001. The inclination distribution of the Kuiper Belt. *Astron. J.* **121**, 2804–2814.

Brunini, A., and J. A. Fernández 1996. Perturbations on an extended Kuiper disk caused by passing stars and giant molecular clouds. *Astron. Astrophys.* **308**, 988–994.

Brunini, A., and J. A. Fernández 1999. Numerical simulations of the accretion of Uranus and Neptune. *Planet. Space Sci.* **47**, 591–606.

Brunini, A., and M. D. Melita 1998. On the existence of a primordial cometary belt between Uranus and Neptune. *Icarus* **135**, 408–414.

Brunini, A., and M. D. Melita 2002. On the accretion of Uranus and Neptune. *Mon. Not. R. Astron. Soc.* **330**, 184.

Chambers, J. E. 1999. A hybrid symplectic integrator that permits close encounters between massive bodies. *Mon. Not. R. Astron. Soc.* **304**, 793–799.

Chiang, E. I., and M. E. Brown 1999. Keck pencil beam survey for faint Kuiper belt objects. *Astron. J.* **118**, 1411–1422.

Collander-Brown, S. J., A. Fitzsimmons, E. Fletcher, M. J. Irwin, and I. P. Williams 2001. The scattered trans-neptunian objects 1998 XY95. *Mon. Not. R. Astron. Soc.* **325**, 972–978.

Danby, J. M. A. 1962. *Fundamentals of Celestial Mechanics*. Willman-Bell, Richmond, VA.

Davis, D. R., and P. Farinella 1997. Collisional evolution of the Edgeworth–Kuiper belt. *Icarus* **125**, 50–60.

de la Fuente Marcos, C., and R. de la Fuente Marcos 2001. Reshaping the outskirts of planetary systems. *Astron. Astrophys.* **371**, 1097–1106.

Duncan, M. J., and H. F. Levison 1997. A scattered comet disk and the origin of Jupiter family comets. *Science* **276**, 1670–1672.

Duncan, M. J., H. F. Levison, and S. M. Budd 1995. The dynamical structure of the Kuiper belt. *Astron. J.* **110**, 3073–3081.

Fernández, J. A., and W. H. Ip 1984. Some dynamical aspects of the accretion of Uranus and Neptune: The exchange of angular momentum with planetesimals. *Icarus* **58**, 109–120.

Ferández, J. A., and W. H. Ip 1996. Orbital expansion and resonant trapping during the late accretion stages of the outer planets. *Planet. Space Sci.* **44**, 431–439.

Gladman, B., J. J. Kavelaars, P. D. Nicholson, T. J. Loredo, and J. A. Burns 1998. Pencil beam survey for faint trans-neptunian objects. *Astron. J.* **116**, 2042–2054.

Gladman, B., J. J. Kavelaars, M. J. Petit, A. Morbidelli, M. J. Holman, and T. J. Loredo 2001. The structure of the Kuiper belt, size distribution and radial extent. *Astron. J.* **122**, 1051–1066.

Gladman, B., M. Holman, T. Grav, J. J. Kavelaars, P. D. Nicholson, K. Aksnes, and M. J. Petit 2002. Evidence for an extended scattered disk. *Icarus* **157**, 269–279.

Greenzweig, Y., and J. J. Lissauer 1990. Accretion rates of protoplanets. *Icarus* **87**, 40–77.

Ida, S., J. Larwood, and A. Burkett 2000. Evidence for early stellar encounters in the orbital distribution of Edgeworth–Kuiper belt objects. *Astrophys. J.* **528**, 531–536.

Jewitt, D., and J. Luu 1993. Discovery of the candidate Kuiper belt object 199 2 QB1. *Nature* **362**, 730–732.

Jewitt, D., J. Luu, and C. Trujillo 1998. Large Kuiper belt objects: The Mauna Kea 8K CCD survey. *Astron. J.* **115**, 2125–2135.

Jewitt, D., H. Aussel, and A. Evans 2001. The size and albedo of Kuiper-belt object (20000) Varuna. *Nature* **411**, 446–447.

Kenyon, S. J., and J. X. Luu 1999. Accretion in the early Kuiper belt. II. Fragmentation. *Astron. J.* **118**, 1101–1119.

Knezévic, Z., A. Milani, P. Farinella, Ch. Froeschlé, and C. Froeschlé 1991. Secular resonances from 2 to 50 AU. *Icarus* **93**, 316–330.

Kokubo, E., and S. Ida 1996. On runaway growth of planetesimals. *Icarus* **123**, 180–191.

Kowal, C. T. 1989. A Solar System survey. *Icarus* **77**, 118–123.

Levison, H., and A. Stern 2001. On the size dependence of the inclination distribution of the main Kuiper belt. *Astron. J.* **121**, 1730–1735.

Malhotra, R. 1995. The origin of Pluto's orbit: Implications for the Solar System beyond Neptune. *Astron. J.* **310**, 420–429.

Melita, M. D., and A. Brunini 1999. The evolution of the Kuiper belt during the formation of the outer planets. In *Evolution and Source regions of Asteroids and Comets, Proc. IAU Colloquium 173* (J. Svoren and E. M. Pittich, Eds.), p. 37. Astron. Inst. Slovack Acad. Sci., Tatranská Lomnica, Slovack Republic.

Morbidelli, A., and G. B. Valsechi 1997. Neptune scattered planetesimals could have sculptured the primordial Edgeworth–Kuiper belt. *Icarus* **128**, 464–468.

Nagasawa, M., and S. Ida 2000. Sweeping secular resonances in the Kuiper belt caused by depletion of the solar nebula. *Astron. J.* **120**, 3311–3322.

Parisi, M. G., and A. Brunini 1999. Constraints to the masses of the large planetesimals. *Planet. Space Sci.* **47**, 607–618.

Sheppard, S. S., D. C. Jewitt, C. D. Trujillo, M. J. I. Brown, and M. C. B. Ashley 2000. A wide field survey for Centaurs and Kuiper belt objects. *Astron. J.* **120**, 2687–2694.

Stern, S. A. 1991. On the number of planets in the outer Solar System: Evidence of a substantial population of 1000-km bodies. *Icarus* **90**, 271–281.

Stern, S. A., and J. E. Colwell 1997a. Accretion in the Edgeworth–Kuiper belt: Forming 100–1000 km radius bodies at 30 AU and beyond. *Astron. J.* **114**, 841–849.

Stern, S. A., and J. E. Colwell 1997b. Collisional erosion in the primordial Edgeworth–Kuiper and the generation of the 30–50 AU Kuiper gap. *Astrophys. J.* **490**, 879–882.

Stevenson, D. J. 1982. Formation of the giant planets. *Planet. Space Sci.* **30**, 755–764.

Stevenson, D. J. 1984. On forming giant planets quickly. *Lunar Planet. Sci.* **XV**, 822–823.

Tegler, S. C., and W. Romanishin, 2000. Extremely red Kuiper-belt objects in near-circular orbits beyond 40 AU. *Nature* **407**, 979–981.

Thommes, E. W., M. J. Duncan, and H. F. Levison 1999. The formation of Uranus and Neptune in the Jupiter–Saturn region of the Solar System. *Nature* **401**, 635–637.

Trujillo, C. A., and E. Brown 2001. The radial distribution of the Kuiper belt *Astrophys. J.* **554**, 95–98.

Trujillo, C. A., and M. E. Brown 2002. A correlation between inclination and color in the classical Kuiper belt. *Astrophys. J.* **566**, L125–128.

Trujillo, C. A., D. C. Jewitt, and J. X. Luu 2001. Properties of the trans-neptunian belt: Statistics of the CFHT survey. *Astron. J.* **122**, 457–473.

Wisdom, J., and M. Holman 1991. Symplectic maps for the N-body problem. *Astrophys. J.* **102**, 1528–1638.

Yu, Q., and S. Tremaine 1999. The dynamics of Plutinos. *Astron. J.* **118**, 1873–1881.